**Journal of the Earth and Space Physics, Vol. 41, No. 4, 2016, PP. 69-76**

# Relationship between head wave amplitudes and seismic refraction velocities to detect lateral variation in the refractor

Nikrouz, R.*

*Assistant Professor, Geology Group, Urmia University, Iran*

*(Received: 30 Dec 2014, Accepted: 02 Jun 2015)*

## Abstract

Refractor ambiguities are big problem in seismic refraction method especially in seismic engineering. There can be hidden subsurface geological phenomena such as hidden faults and shear zones which are not simply predicted by the travel-time graph or some geophysical methods. Head wave amplitudes are used to show the resolution of refractor ambiguities and the existence of anisotropy in complex geological area. Wave amplitude is proportional to the square root of energy density; it decays as 1/r. In practice, velocity usually increases with depth, and causes further divergence of the wave front and a more rapid decay in amplitudes with distance. Amplitudes measured from first peak to first trough and corrected for geometric spreading, can be demonstrated some subsurface information such as anisotropy. Meanwhile, amplitudes are not commonly study by researchers in seismic refraction studies, because of being the very large geometric spreading components due to variations related to wave speeds in the undulated refractor. The variations in amplitudes are described with the transmission coefficient of the Zoeppritz equations. This variation in velocity and density produces head wave amplitude and head coefficient changes in refractor, even with refractors exhibiting large variations in depth and wave speeds. The head coefficient can be approximately calculated by the ratio of the specific acoustic impedance in the overburden layer in the refractor. This study shows that there is a relationship between the amplitude and the seismic velocity which the lower the contrast in seismic velocity and/or density, the higher the amplitude and vice versa.

**Keywords:** Acoustic impedance, Head wave amplitudes, Seismic refraction, Seismic velocity.

## 1. Introduction

The calculation of seismic wave amplitudes is not a simple matter and the analysis of amplitudes and related information such as attenuation is one aspect of the refraction method where major gains can be achieved with relatively minor efforts (Palmer, 1986). In the recent years, there has been significant research on the use of amplitude in the seismic refraction survey. Whereas seismic data were once commonly acquired along widely spaced profiles, it is now more usual to obtain seismic data along numerous closely spaced traverses. As a result, the spatial sampling is now comparable in both horizontal directions and the greater resolution has greatly improved the interpretation of complex geological features (Nikrouz, 2005). The fundamental problem facing two-dimensional (2-D) seismic methods (Refraction and Reflection) is the fact that most geological targets are three-dimensional. In the past, two-dimensional methods have attempted to address this problem by locating lines with the strike and dips of the major features in mind, minimizing but rarely eliminating the effect of the third dimension (Brown, 1996). In many cases, 2D methods can provide an incorrect rather than an incomplete picture of the subsurface structure. The differences can be explained by the fact that the geological targets can vary significantly in both horizontal directions, thereby requiring the adequate spatial sampling obtained by 3D methods. In other words, the incorrect subsurface structure can often be the result of spatial aliasing (Nikrouz and Palmer, 2004). To resolve this ambiguity, amplitude analysis can help interpreter have more information about subsurface refractor.

Refractor ambiguities are big problem in seismic refraction method especially in seismic engineering surveys. There can be hidden subsurface geological phenomena such as hidden faults and shear zones which are not simply predicted by the travel-time graph or some geophysical methods (Nikrouz, 2006). Head wave amplitudes are

*Corresponding author: E-mail: r.nikrouz@urmia.ac.ir

used to show the resolution of refractor ambiguities and the existence of anisotropy to generate pseudo-geological maps. The geological map traditionally has been one of the most important domains for visual summarizing of geological information. The reasons for this are that geological data have traditionally been acquired through examination of various sites, exposures, and etc. on the earth's surface and, therefore, the geological map is a self-evident summary of these activities. Furthermore, many geological processes take place in the near surface region, and therefore, it is frequently more convenient to conceptualize the horizontal domain (Nikrouz, 2005).

Amplitudes of refracted arrivals have always been observed when processing seismic data. In the past, the researchers were mainly concerned about their existence and not their magnitude since the objectives of seismic surveying were structural (Brown, 1987). Amplitudes are not commonly used in seismic refraction studies, because the very large geometric spreading component is dominated any variations related to wave speed in the refractor. It should be noted that the processing of the first-arrival amplitudes are useful in seismic refraction studies because they can indicate the gross velocity model and facilitate the convenient detection of the amplitude variations related to changes in the seismic velocities in the refractor (Palmer, 2001a). As Palmer (2001b) concluded, the higher the contrast in the refractor wave speed, the lower the head wave amplitude and vice versa. The expression to calculate the amplitude of the head wave for a thick refractor with a plane horizontal interface is presented by Heelan (1953) and Werth (1967) as below:

$$\text{Amplitude} = KF(t)/(rL^3)^{1/2} \quad (1)$$

where K is the head coefficient (constant dependent upon the elastic parameters), which is a function of the contrasts in seismic velocities and/or densities between the upper layer and the refractor. F (t) is the displacement potential of the incident pulse, r is the source to receiver distance, and L is the distance the wave has traveled within the refractor.

The geometric spreading is defined as the component of the variation in the amplitude of the refracted arrivals which can be attributed solely to the shot-to-receiver distance (Palmer, 2006):

Geometric spreading component =

$$1/((rL^3)^{1/2}) \quad (2)$$

For most shallow seismic refraction surveys, the geometric spreading component is dominated on the head wave amplitude.

Thus, it must be removed in order to detect the amplitude variations related to changes in refractor. The expression for K given by Werth (1967) is:

$$K = \frac{2\rho\chi\gamma[\lambda_1(1+2m\gamma^2)+\lambda_2(\rho-2m\gamma^2)]^2}{(1-\gamma^2)^{1/2}[\gamma^2(1+2m\gamma^2-\rho)+\rho\chi\lambda_2+\chi\lambda_1(1+2m\gamma^2)^2]^2} \quad (3)$$

where,

$\gamma = V_{P1}/V_{P2}$

$\rho = \rho_1/\rho_2$

$m = \rho(V_{S1}^2/V_{P1}^2) - (V_{S2}^2/V_{P1}^2)$

$\chi = (1-\gamma^2)^{1/2}$

$\lambda_1 = (V_{P1}^2/V_{S1}^2 - \gamma^2)^{1/2}$

$\lambda_2 = (V_{P1}^2 + V_{S2}^2 - \gamma^2)^{1/2}$

$V_{P1}$ = compressional wave speed in upper media

$V_{S1}$ = shear wave speed in upper media

$\rho_1$ = density in upper medium, and similarly for the lower medium 2.

For strong contrasts in wave speeds, i.e. for

$$\gamma \longrightarrow 0, \qquad K\rho\gamma = \rho_1 V_{p1}/\rho_2 V_{p2} \quad (4)$$

The evaluation of K for a selected set of elastic parameters shows that the amplitude can be decreased as the contrast in the seismic velocity between two media is increased (Cerveny and Ravindra, 1971; O'Brien, 1967). Meanwhile, as Palmer (2001a) showed the simplified relationship between amplitudes and the specific acoustic impedances takes no account of variations in shear wave speeds, attenuation, or diffractions which constitute a large proportion of the refracted signal with irregular interface.

Furthermore, Palmer (2001a) indicated that the head coefficient is proportional to the ratio of the specific acoustic impedance, which is the product of the seismic velocities and densities, in the overburden and the refractor. Therefore, if the detailed lateral variations in the refractor velocities can be

resolved with the travel time data, then it is likely that the derivation of a model of the lateral variations are in the bulk in-situ densities from the amplitude data.

## 2. Data acquisition

The study area is situated on the southern margin of the Gunnedah and Surat Basin both of which overly the western margin of Lachlan Fold Belt, in the Spicers Creek Catchment (NSW), in southeastern Australia. The seismic data were recorded with the Australian National Seismic Imaging Resources (ANSIR) 360-trace ARAM-24 seismic system and IVI MiniVibrator. Survey geometry (Fig. 1) consisted of four parallel receiver lines 10 m apart. Each line is consisted of 29 three-component geophones (GS-20DM, natural frequency 14 Hz) at 5 m intervals and 20 m vibrator shot point separation. The Minivib can be configured in the field to generate P-, SH and SV waves. The accuracy in setting out the receiver and source lines was generally quite good. This can be seen in the GPS readings, which were taken at both ends and at the centre of each receiver line at every source point. After setting up the recording spread, all the components were checked from the recording truck. This process involved test of the response of each geophone element to ensure that they were all connected to each other with correct functioning, battery power level checking, and amplifiers testing. Figure 2 shows an example of P-wave shot record.

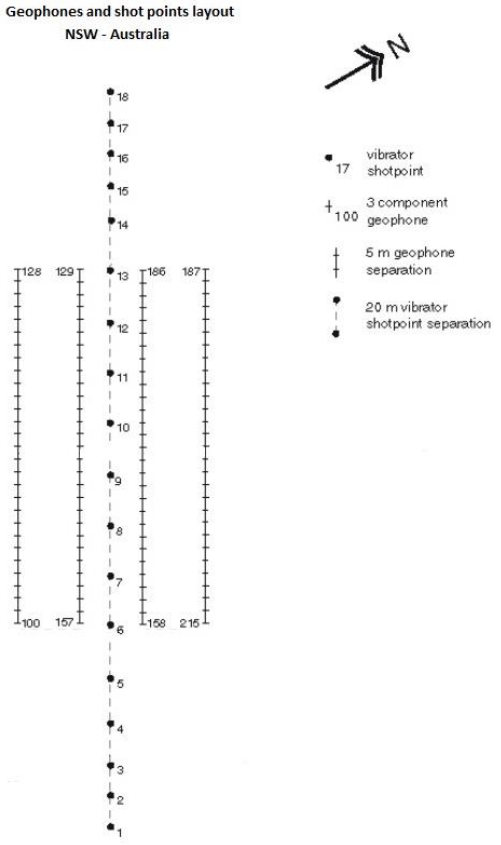


**Fig. 1.** Geophones and shot points layout (NSW-Australia)

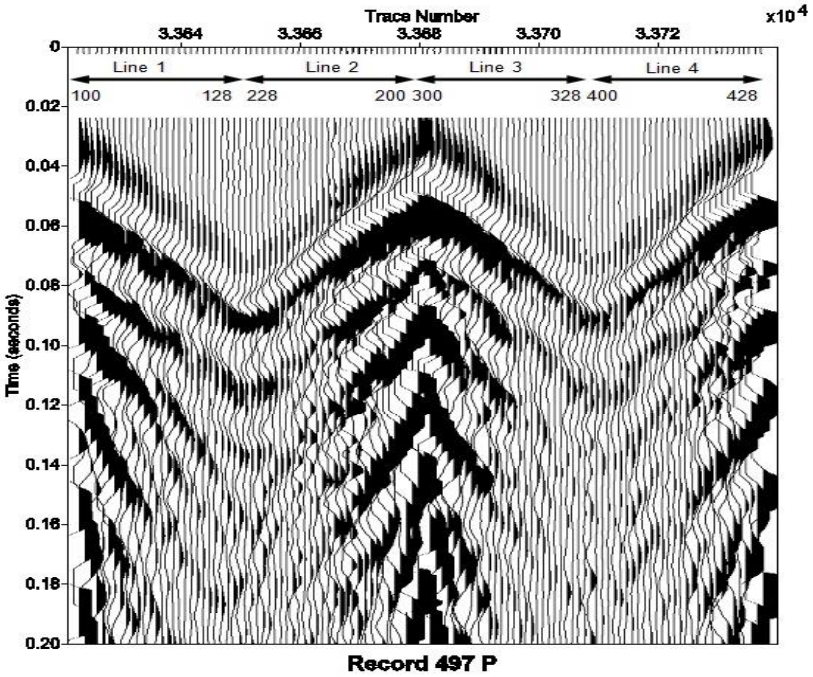


**Fig. 2.** Example of P-wave record

## 3. Data processing

Data were processed by Microsoft Excel, surfer, Visual-SUNT, Rayfract and seismic Un*x program. Seismic Un*x (SU) program was developed by the centre for wave phenomena at the Colorado School of Mines. These software packages were used to generate three-dimensional images, calculate velocity ratios of waves, pick the first-arrialtraveltimes, head wave amplitudes, display the shot records, process the full shot records and wave eikonaltraveltime (WET) tomography images.

It should be mentioned that before picking first arrivaltimes and head wave amplitude, two procedures which muted and killed traces were performed to improve the first-arrival picks. By using the muting, traces can be zeroed out either before or after the first-arrivals, whilst the killing enables removal of entire traces. The muting was done by the shell script 'mute' and the killing by the SU command 'sukill'. The muting and killing traces can improve the quality of first-arrival picking. Figure 3 shows the original cross line horizontal component shot record with considerable noise and dead traces and the same shot record after the killing and muting above the first-arrivals.

The determination of the seismic velocities in the refractor was a four-stage process. In the first stage, the traveltime from different source points were phantomed then averaged. This process generated traveltimes which were largely free of picking random errors and, therefore, they were quite accurate. In the second stage, the time-depth algorithm of the Generalized Reciprocal Method (GRM) was used to generate corrections for any near-surface irregularities. These corrections minimized the likelihood of generating artefacts related to the near-surface irregularities. In the third stage, the velocity analysis algorithm of the GRM was evaluated then averaged over a range of XY values. This averaging process effectively minimized the likelihood of generating artefacts related to variations in the depth to the refractor. In the final stage, the seismic velocities in the refractor were obtained by linear regression. The velocities for all wave-types (P, SV and SH) are shown in Figure 4.

In order to recognize any amplitude variations related to head coefficient, it was necessary to reduce the effect of geometrical spreading. To do this, we computed the amplitude product for each forward and reverse shot pair (Palmer, 2001b). The product of the forward and reverse shot amplitudes compensates for the effects of geometric spreading and dipping refractors (Palmer, 2003a, b). The amplitude product was calculated only for the P-waves since the S-waves did not show good consistency.

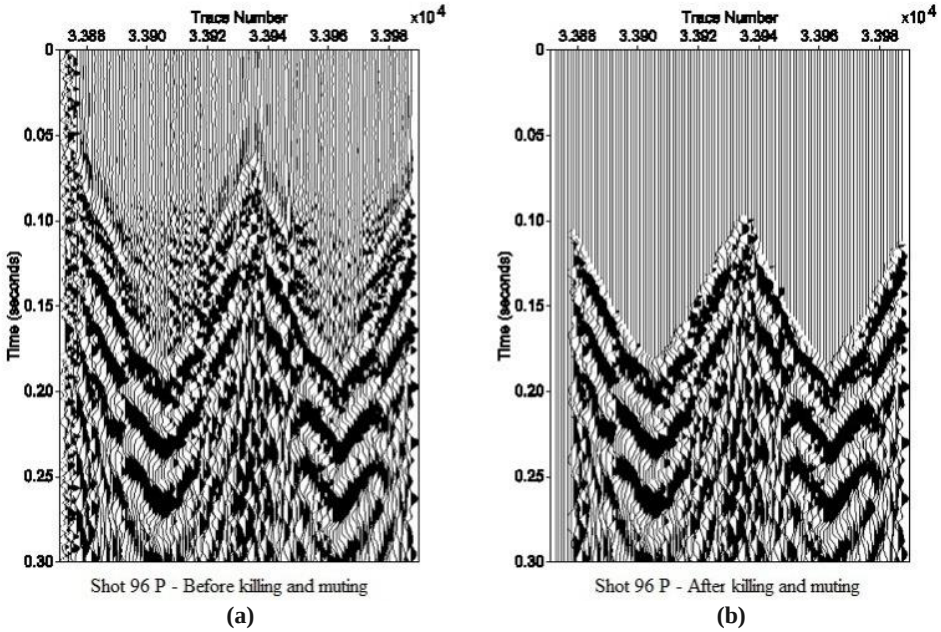


**Fig. 3.** (a) Shot record before killing and (b) muting and after killing and muting

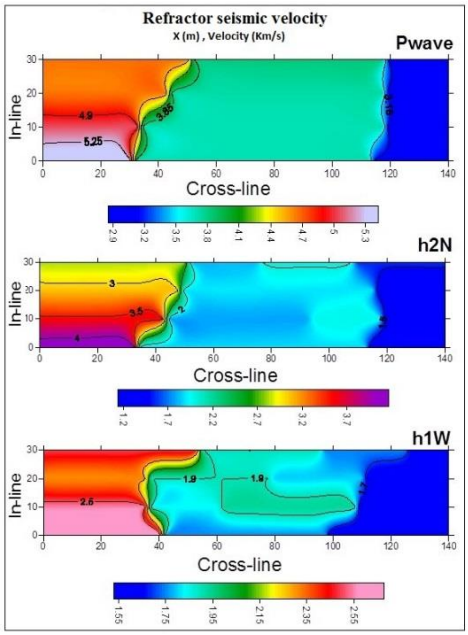


**Fig. 4.** Refractor seismic velocity for P-SH (h2N) –SV (h1w) waves.

The effectiveness of this operation can be seen in Figure 5. As it can be seen forward and reverse distance P-wave amplitudes for shots 5 and 14 was calculated with 1/x, 1/x^2 and 1/x^3. The large geometric spreading component dominates. Meanwhile, the effects of geometric spreading have been reduced. The product of this shot pair as well as a number of other offset shot pairs is shown in Figure 6. There are gross similarities in the shape of the amplitude products for all the shot pairs, suggesting that the variations are related to variations in the seismic velocities in the refractor.

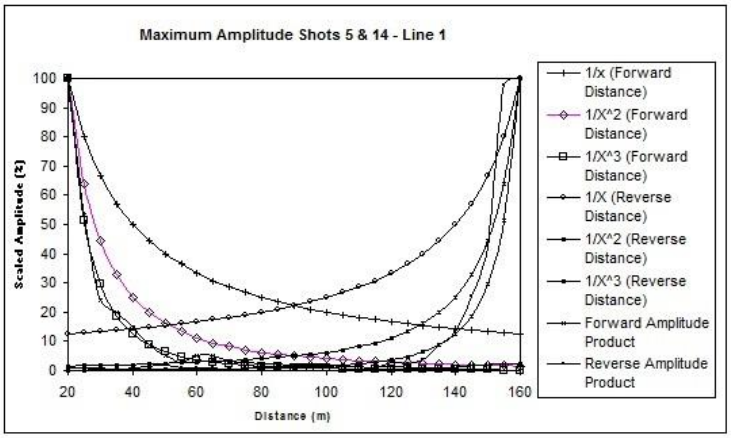


**Fig. 5.** Forward and reverse distance P-wave amplitudes (with calculating 1/x, 1/x^2 and 1/x^3).

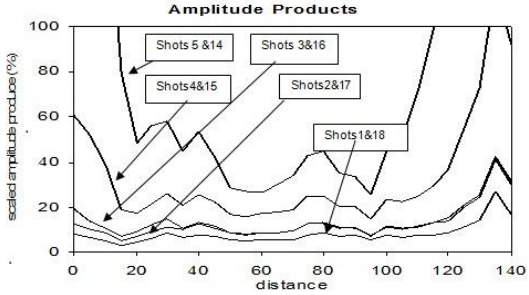


**Fig. 6.** The product of forward and reverse amplitudes for various offset shot pair.

## 4. Traveltime tomography

Wave Eikonal Traveltime (WET) tomography was used to generate a velocity depth section in every line for P-wave. WET tomography accommodates multiple signal paths. It contributes to each first break and is an efficient computational and robust geophysical method. WET inversion is a high frequency traveltime tomographic method. It is an efficient computational method, being an order of magnitude faster than wave equation traveltime inversion since only solutions to the eikonal equation are involved.

The first step was to generate starting model by using both one and two dimensional inversion methods. The delta-t-v method was used to generate 1D starting models (Gebrande and Miller, 1985). This method is a pseudo tomographic method that yields one-dimensional velocity profiles for each common midpoint (CMP). This tuning ray inversion method delivers continuous depth vs. velocity profiles for all profile stations. The starting models were then refined with WET tomography until the modeled traveltimes is ideally matched with the field traveltimes. The starting models were then refined with WET tomography until the modeled traveltimes were ideally matched with the field traveltime.

Figure 7 shows the final section from WET tomography. The section generated using 1D starting model with multiple layers off assumed constant vertical velocity gradients. Figure 8 shows the section generated using 2D starting model derived from the GRM. Despite the large differences in the sections, both fit the field data to acceptable accuracy.

## 5. Interpretation

The theoretical basis for the derivation of in-situ densities from head wave amplitudes is relatively straightforward (Palmer et al., 2005). Palmer (2001c) demonstrates that the product of the forward and reverse head wave amplitude compensates for geometric spreading and that the result is proportional to the head coefficient. The head coefficient is analogous to the transmission coefficient of the Zeoppritz equation and it describes the head wave amplitude in terms of the petrophysical properties in the two media.

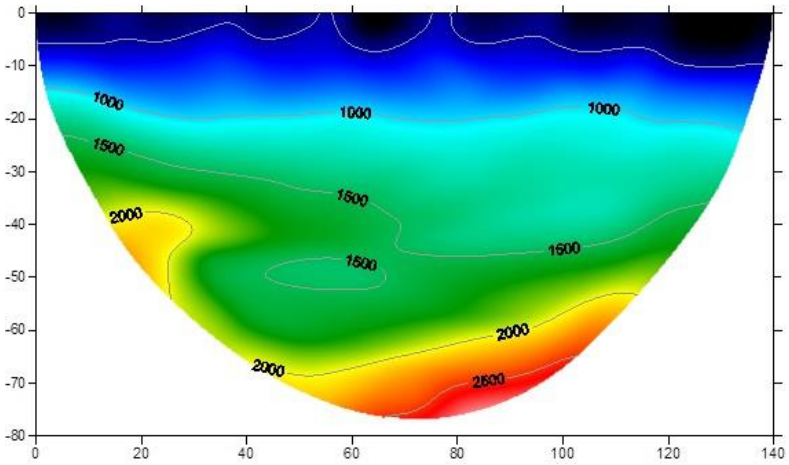


**Fig. 7.** Final section from WET tomography

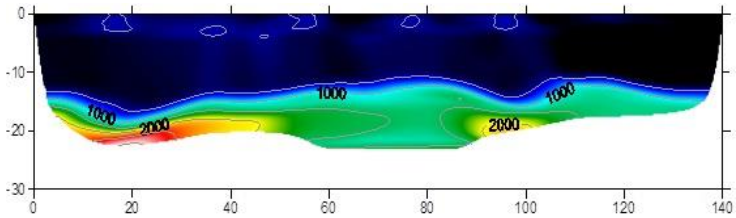


**Fig. 8.** The section generated using 2D starting model (with GRM)

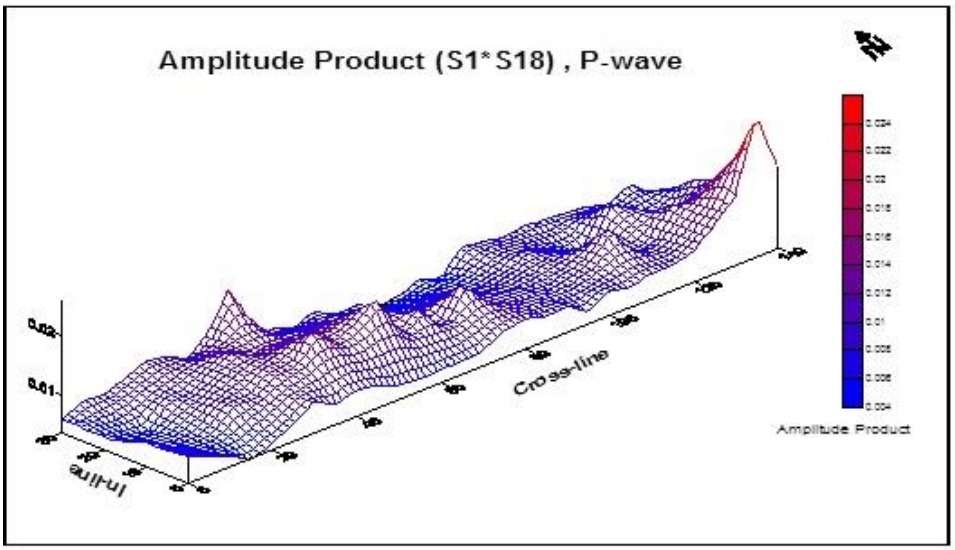


**Fig. 9.** Wireframe map of amplitude product for P-wave

Figure 5 shows the large amount of geometric spreading from a shot pair 20 m from the receiver spread, with the amplitudes decaying much faster than the reciprocal of the distance squared as in Figure 6. The removal of the geometric spreading component is the most effective between 20 and 100 m. There are also gross similarities in the shape of the amplitude products for all the shot pairs. This suggests that the variations are related to the head coefficient and hence to the variations in the seismic velocities in the refractor.

Figure 9 is the wireframe map of amplitude product with the geometric effect correction being applied. The map can be divided into three regions. A region of high amplitude product exists between cross-line among 0 to 60 m; a region of low amplitude product exists between cross-line among 60 m to 100 m; and a region of high amplitude product exists between cross-line among 100 m to 140 m. The presence of these regions suggests that variations in amplitudes are associated with velocity changes (Figs. 4, 7, 8) in the refractor. A considerable degree of noise is also evident on the amplitude products and is related to lateral variations in the near surface layers. The low amplitude between cross-line 0 to 20 m and high amplitude between cross-line 100 m to 120 m are possibly due to near surface effects in the study area.

In general, figures show the lateral changes in refractor in term of velocity for all type-waves. For all wave-types the boundary between the region of low and high seismic velocity is quite distinct. The first region is between cross-line 0 to 40 m, the second between 40 m to 110 m, the third between 110 to 140 m.

## 6. Conclusions

Although, a detailed analysis of the head wave amplitudes did not generate useful results, the fact that the head wave amplitude is a function of the densities, as well as the seismic velocities, suggests that the joint inversion of seismic refraction traveltimes and head wave amplitudes should facilitate the determination of both seismic velocity and density models.

As it is usually the case, increased numbers of recording channels would have been beneficial. The consistent zoning of amplitude and refractor velocities for all wave-types (P-SH-SV) is compelling evidence for genuine lateral lithological changes within the bedrock especially for the second mentioned area (40 m to 110 m). These seismic velocities models together with the amplitude variations suggest a narrow shear zone at the second region (cross-line 40 to 110 m) characterized by low seismic velocities and increased depth of weathering. This variation in velocity and density produces head wave amplitude and head coefficient changes in refractor, even with refractors exhibiting large variations in depth and wavespeeds. As a result, the higher the contrast in the refractor wave speed the lower the head wave amplitude and vice versa.

**Acknowledgements**

Author is thankful to Dr. Derecke Palmer for his keen supervision and David Johnston and the ANSIR team (NSW-Australia) who made it possible to gather seismic data.

**References**

Brown, A. R., 1987, The value of seismic amplitude, The Leading Edge, October 1987, 30-33.

Brown, A. R., 1996, Interpretation of three-dimensional seismic data, AAPG Memoir, 42.

Cerveny, V. and Ravindra, R., 1971, Theory of seismic head waves, University of Toronto Press.

Gebrande, H. and Miller, H., 1985, Refraction seismology, In: Bender, F. (Ed), Applied Geosciences, methods of applied geophysics and mathematical procedures in geosciences, F. Enke publishing house, Stuttgart.

Heelan, P. A., 1953, On the theory of head waves, Geophysics, 18, 871-893.

Nikrouz, R., 2005, Three-dimensional (3D) three-component (3D) shallow seismic refraction surveys across a shear zone associated with dryland salinity at the spicers creek catchment, PhD thesis, School of Geology, NSW, Sydney, Australia.

Nikrouz, R., 2006, Near-surface corrections with the GRM, 17th International Geophysical Congress & Exhibition by CGET, 14-17 Nov., Ankara-Istanbul.

Nikrouz, R. and Palmer, D., 2004, 3D 3C seismic refraction imaging of shear zone sources of dryland salinity, 17th Geophysical Conference and Exhibition, 15-19 August, Sydney, Australia.

O'Brien, P. N. S., 1967, The use of amplitudes in seismic refraction survey, in: Musgrave, A. W. (Ed), Seismic refraction prospecting, Society of Exploration Geophysicists, Tulsa.

Palmer, D., 1986, Refraction seismics, the lateral resolution of structure and seismic velocity, Geophysical Press.

Palmer, D., 2001a, Resolving refractor ambiguities with amplitudes, Geophysics, 66, 1590-1593.

Palmer, D., 2001b, Digital processing of shallow seismic refraction data with the refraction convolution section, PhD thesis, School of geology, NSW, Sydney, Australia.

Palmer, D., 2001c, Imaging refractors with the convolution section, Geophysics, 66, 1582-1589.

Palmer, D., 2003a, Application of amplitudes in shallow seismic refraction inversion, ASEG 19th Geophysical Conferences and Exhibition, Adelide.

Palmer, D., 2003b, Processing and interpreting shallow seismic refraction data with the GRM and the CRM, unpublished: university of New South Wales, Sydney, Australia.

Palmer, D., 2006, Refraction travel time and amplitude corrections for very near-surface in homogeneities, Geophysical Prospecting, 54, 589-604.

Palmer, D., Nikrouz, R. and Spyrou, A., 2005, Statics corrections for shallow seismic refraction data, Exploration Geophysics, 36, 7-17.

Werth, G. A., 1967, Method for calculating the amplitude of the refraction arrival, in: Musgrave, A. W. (Ed), seismic refraction prospecting, Society of Exploration Geophysics, 119-137.